

# Investigation The Hydroxyapatite Coatings On Titanium Alloys Using Magnetron - Sputtered Process And Differentiate Between Single And Triple Layers.

**Dunya Abdulsahib Hamdi**

Department of mechanical Engineering college,  
Al Nahrain University  
Baghdad ,Iraq  
School of Engineering and Information Technology,  
Murdoch University,  
Murdoch,6150WA, Australia  
dunia\_sh\_7@yahoo.com

**Kwangsoo NO**

Department of Materials Science and Engineering,  
Korea Advanced Institute of Science and Technology  
Daejeon, South Korea  
kaistksno@kaist.ac.kr

**L.Thair**

directoral of Research and Nuclear applications,  
Ministry of Science and Technology  
Baghdad ,Iraq  
Phythair2011@gmail.com

**Zhong Tao Jiang**

School of Engineering and Information Technology,  
Murdoch University,  
Murdoch,6150WA, Australia  
z.jiang@murdoch.edu.au

**Jaegyu Kim**

Department of Materials Science and Engineering,  
Korea Advanced Institute of Science and Technology  
Daejeon, South Korea  
kimjaegyu@kaist.ac.kr

**Thamir Abdul- Jabaar Jumaee**

department of physics, college of Sciences ,  
Al Nahrain university,  
Baghdad ,Iraq  
drthamir05@yahoo.com

**Abstracts** -Titanium and its alloys are used, because of their high mechanical properties, chemical stability, and biocompatibility. Due to its poor osteoconductive properties, coating of bioactive hydroxyapatite HAp ( $\text{Ca}_{10}(\text{PO}_4)_6(\text{OH})_2$ ), which has similar chemical and crystallographic structure to the main inorganic phase of human bone tissues. Reaction bonding process. Scanning Electron Microscope (SEM), Energy Dispersive X-ray Spectrometer (EDS) and X-ray Diffraction (XRD) were employed to characterize the titanium substrate and as-prepared coatings. From SEM, the interfacial bonding strength of the sintered composite coating was tested. Results show that the tripe form composite coating can be easily sintered with no cracks and decomposition at  $600^\circ\text{C}$ , the bonding strength to the substrate is significantly improved compared with the single HAp coating. The EDS result, A concentration weight Ca , P increasing with time of working sputtering. The results of the X-ray diffraction pattern revealed that the sputtering shows a thin layer coating contain nano size crystals. The *in vitro* electrochemical measurement results also indicated there is improvement in corrosion resistant of single layer and triple layer coated compare with the uncoated as follows, 30716, 508276 and 23176  $\Omega(\text{ohm})$  respectively this improvement related triple layer HAp using RF sputtering .

**Keywords—Biomaterial; sputtering; coating; Corrosion**

## I. INTRODUCTION

Surfaces modification of Ti, Ti-alloys or any other alloys are used to improve the implant-tissue Osseo integration and to increase bioactivity of such materials using different methods, e.g., wet and electro chemical treatment method [1], sol-gel method [2], electrophoretic deposition (EPD) [3][4] [5], high power lasers deposition [6], plasma spray coating process [7][8], RF plasma sputtering deposition method [9] [10] [11] and reactive plasma sputtering [12] etc. Films using magnetron sputtering technique are of high-quality, high density , high adhesion , good thickness under controlled uniformity over a large area obtained at a low substrate temperature , meeting the requirements of grain size distributions and, crystallinity, as needed for the desorption in body fluids [13]. The interface between the implant materials and hard tissue possesses reactions at the interface various depend on the types of materials [14] to improved biocompatibility, Ti implants provided by bioactive ceramic such as the hydroxyapatite (HA,  $\text{Ca}_{10}(\text{PO}_4)_6(\text{OH})_2$ ). HA have chemical stability and values of the elasticity modulus close to the mineral phase of natural bone apatite also the excellent osteoconductivity makes it an ideal scaffold for the formation of new bone [13]. HA grow with different types occurrence in biological dental, soft-tissue deposits, arthritic cartilage, bone, urinary stones,

Atheros. It has been sought to induce apatites formation on the metallic surface in the living body, because this layer has been dissolved in surrounded body fluid due to biological processes, many attempts have been made to form mid layer on the Ti substrate using various material, such as  $\text{TiO}_2$ ,  $\text{Al}_2\text{O}_3$ ,  $\text{SiO}_2$  to improve the bonding capability of the HA layer with respect to the Ti substrate and prevent the Ti substrate from becoming corroded [15]. The thermal expansion coefficient of Ti alloy substrate ( $\text{Ti} = 8.7 \times 10^{-6}/\text{K}$ ), is much lower than that of HAp ( $\text{HAp} = 13.6 \times 10^{-6}/\text{K}$ ), this large different in thermal expansion mismatch leads to the formation of cracks in coatings. The addition of  $\text{TiO}_2$  with relatively lower thermal expansion coefficient ( $\text{TiO}_2 = 7.249 \times 10^{-6}/\text{K}$ ), create strong bound with substrate with .The  $\text{Al}_2\text{O}_3$  had high hardness and thermal expansion coefficient ( $\text{Al}_2\text{O}_3 = 8.2 \times 10^{-6}/\text{K}$ ) also agreement with  $\text{TiO}_2$ , all these will lead to a thermal expansion mismatch reduction between HAp and Ti alloy[15,16]. The cpTi alloy have high corrosion resistance used in dental implant, this study was performed to fabricate an HA as single layer and HA/ $\text{Al}_2\text{O}_3$ / $\text{TiO}_2$  as triple layer coating on the cpTi substrate. The HA layer is expected to enhance the bioactivity and osteoconductivity during the initial stage following implantation, by acting as an outer coating layer the  $\text{Al}_2\text{O}_3$ / $\text{TiO}_2$  as inner layer. Simple chemical SBF treatments the samples after coated could induce apatite formation on the surfaces of samples.

## II. RAW MATERIALS AND EXPERIMENTAL TECHNIQUE.

Titanium alloys rods, (cpTi) GR2 ASTM F67 has the composition (99.3%wTi, 0.30 %w Fe, 0.080 %wC, 0.03%wN, 0.25%wO, 0.015%wH). The specimens of cpTi alloy were used as substrates in plasma sputtering experiment with a circular shape (2 cm diameter and a 1.8 mm thickness) dimensions. The specimens' alloys were grained SiC paper in the flowing steps :( 120, 180, 240, 320, 500, 600, 800, 1000 , 1200 ,1800 and 2500 $\mu\text{m}$  of grain size) and polished using (Struers- DAP-U system, Denmark), etching the samples and ultrasonically were cleaned. Three types targets in the form of powder are used :  $\text{TiO}_2$ ( has 4~5 $\mu\text{m}$  of particle size with purity (99.995%) ) ,HA( has 2 $\mu\text{m}$  particle size , with purity 99.9) and  $\text{Al}_2\text{O}_3$ ( has 1 $\mu\text{m}$  of particle size with purity 99.999%). The RF magnetron sputtering device was situated in a vacuum chamber  $1 \times 10^{-7}$  Torr, operation frequency of the rf generator 13.65MHz , Ar sputtering gas . Before the thin film deposition, pre-sputtering was carried out for about 5 min at Ar gas with sputtering pressure at first  $2 \times 10^{-2}$  Torr expected to remove the surface oxidation and contamination of the target and working pressure  $5.5 \times 10^{-3}$  Torr. Deposition time was controlled to obtain a uniform film thickness, the distance was change between target and substrates with conditions works are tabulated for each experiment. All the samples was annealing by using furnace at 600 °C for 1 hour, 2 $^\circ$ /min (all process take 11 hours) under the air.

HA crystalline structure is coated on Titanium alloys substrates were scanned at depth 1 $\mu\text{m}$  using an XRD,20 KV,2mA,0.04KW with a monochromatic CuK (1.54056 Å) radiation occupying a scan speed of 2 $^\circ$  per minute and a step Scan ratio 0.01.Information on elemental composition and concentration at depth 100nm were analysed used (EDS- PHILIPS XL series).

morphology of thin film HA coating as single and third layer were analysed used (scanning electron microscopy (SEM- HITACHI 5- japan 4800). and in order to avoid electrical charging due to low electrical conductivity of coated surfaces.

The elemental and chemical analysis of surface samples at penetration depth 2-5nm was performed using (XPS- KRATOS AXIS ULTRA DLD) monochromatic radiation scanned AlK $\alpha$  X-rays (  $h\nu=1486.6$  eV) were used to excite the photoemission. The sample analysis is conducted in a vacuum chamber,  $\sim 10^{-10}$  Torr controlled and analysis by (CASA lab software version 10.2x).

*In vivo* test, was investigated from results corrosion behaviour of the implant coated surface with different thickness in SBF solution suggested by Kokubo [17] consisted of 7.9949 g NaCl, 0.3528 g  $\text{NaHCO}_3$ , 0.2235 g KCl, 0.147 g  $\text{K}_2\text{HPO}_4$ , 0.305 g  $\text{MgCl}_2 \cdot 6\text{H}_2\text{O}$ , 0.2775 g  $\text{CaCl}_2$ , 0.071 g  $\text{Na}_2\text{SO}_4$  in 1000 ml distilled water and was buffered to pH 7.4 at 25 $^\circ\text{C}$ , compared with the corrosion behaviour of uncoated implant specimen. The electrochemical measurements were carried out using potentiostat /galvanostat (Biological since instrument EN61010 )provided with electrochemical interface controlled by( EC lab software version 10.2x).All the potential measurements were made with reference Ag Ag/Cl to a saturated calomel electrode (SCE). Platinum was used as control electrode. The corrosion resistance evaluate by electrochemical techniques, namely, OCV -Open Circuit Voltage consists in a period during which no current can flow and no potential can be applied to the working electrode, LSV-Linear Sweep Voltammetry measurements in hydrodynamic steady-state conditions and EIS-Electrochemical Impedance measurements

The Alpha-Step IQ Profiler is a computerized, high-sensitivity surface profiler that measures step height in a variety of applications, used to measure the thickness of thin film.

### A. Single Layer Hydroxyapatite

The cpTi were coated with HA, conditions works are tabulated in Table 1

**Table 1.** Deposition conditions work of HA coated as a single layer onto titanium substrates using RF sputtering technique.

NO. of Experiment	1	2	3	4
Power (W)	150	150	150	150
Working Pressure (Torr)	$5.5 \times 10^{-3}$	$5.5 \times 10^{-3}$	$5.5 \times 10^{-3}$	$5.5 \times 10^{-3}$
Heat substrate. (°C)	300	300	300	300
Distance between target & substrate (cm)	7	7	7	7
Time of working (hour)	2	4	7	10

**B. Triply layers Titania-Alumina-Hydroxyapatite**

The cpTi substrate were coated with  $TiO_2-Al_2O_3$ -HA targets, started with  $TiO_2-Al_2O_3$  as the first and second layer respectively, two hours run for each targets on the substrates at 7 cm distance from targets, then using HA target to deposited as the third lyre on  $TiO_2-Al_2O_3$  thin film for different time deposition, conditions works are tabulated in table 2.

**Table 2.** Deposition conditions work of HA coated as third layer onto the cpTi substrate using RF sputtering technique.

NO. of Experiment	1	2	3
Power(W)	150	150	150
Working Pressure (Torr)	$5.5 \times 10^{-3}$	$5.5 \times 10^{-3}$	$5.5 \times 10^{-3}$
Heat substrate. (°C)	300	300	300
Distance between target & substrate (cm)	7	7	7
Time of working (hour)	2	4	7

**III. RESULTS AND DISCUSSION**

The surface modification of samples were analysis at different depth due to different techniques to discover the concentration, behaviour the elements and the thickness of thin film such as XRD, EDS, SEM, XPS methods and corrosion tests.

**A. X-ray Diffraction**

X-ray diffraction (XRD) analysed the cpTi, Ti6Al4V substrates were coated with HAP thin film as single and triple layer.

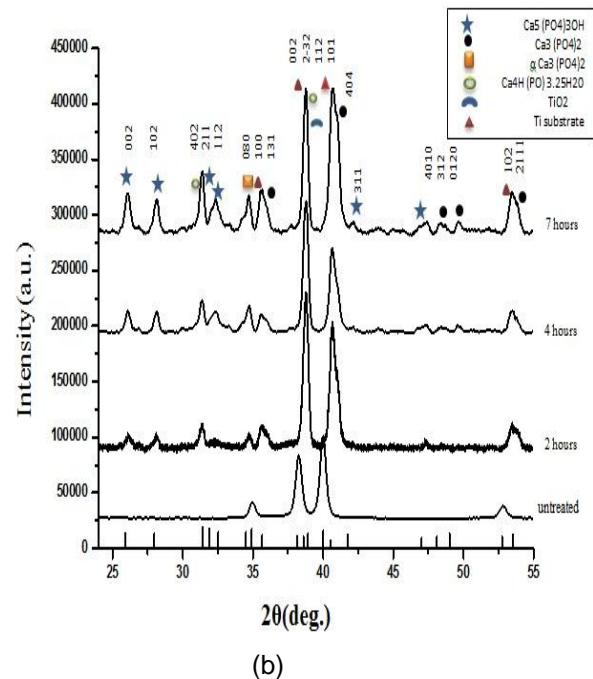
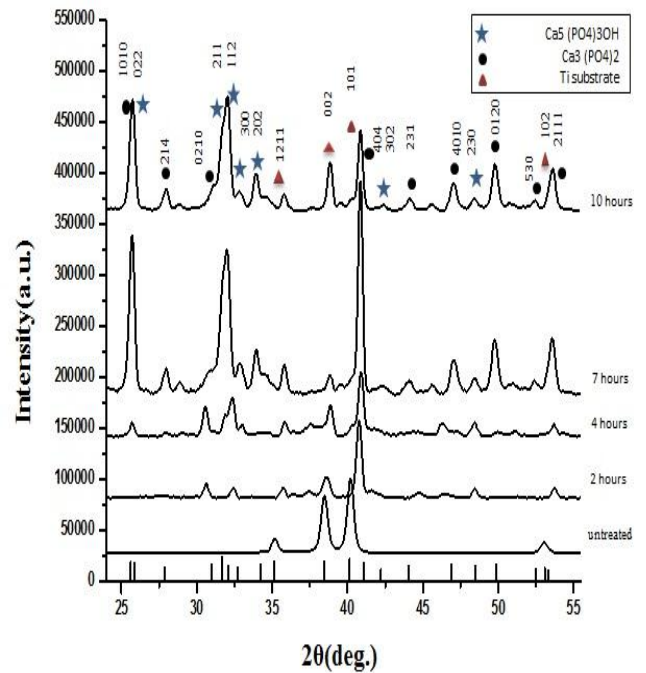


**Figure 1.** XRD pattern confirming the presence grow of single HAP on surface cpTi alloy as (a) single and (b) triple layer for (2,4,7,10) hours.

The X-ray diffraction pattern viral that there is more than one peaks of HAP confirmed for other calcium phosphate crystals and the intensity of thin film increasing with increasing the time of work for HAP coating cpTi and Ti-6Al-4V alloys and reduce in intensity of Ti alloy substrates. Thermal treatment at 600°C show crystalline phase but there is shifting of all peaks toward higher two theta degrees, this result because the heat effect and shear with peaks of thin film coating cpTi and Ti-6Al-4V alloys. From figure (1-a) for 7 hours working time HAP coated on cpTi(101),



the peak intensity increasing because the thickness of thin film increasing which represent in shear peak of (CP) (404). The diffraction angles of the Ti (102) peaks shifted from their original position by reduce in intensity with increasing working time (2 and 4 hours). HAp coated caused by dissolution of oxygen but for working time (7 and 10 hours), the intensity increasing because (102) peak become shear with (2111) peak (CP).

For 10 hours working time the HA peaks intensities increased, there was an improvement in crystallization, strong HAp (112), (211) and (002) with a strong HA (112) overlapping with (211) and preferred orientation suggesting that high coating and chemical reaction between the different components. The (002) HAp peak around 26° was stronger compared to (112), (211) HAp peaks around 32° for the HA coating on cpTi alloy. When the particle size reduce this means the number of particles increase so that the intensity of the peak increase.

The Triple-layered coating consisted of alternating layers of TiO<sub>2</sub>, Al<sub>2</sub>O<sub>3</sub> coated on Ti alloys, followed by depositing a HA as the third layer. From figures (1-b), it is reasonable that phase composition of the coating detected by XRD was include Al<sub>2</sub>O<sub>3</sub>, Ti composition and almost contributed from consisted of a mixture or joint peaks grow of (HA, OCP, CP and α TCP) coatings crystal structure. Approximately the XRD behaviour for triple layer HAp coated is similar to behave for single layer, there is shift for all Ti alloys peaks toward higher two theta degrees and the intensity (002), (101) and (102) peaks this increasing with increasing time of working starting from time of work (2 hours) due to the thickness of thin film increasing which represent in shear peak (2-32), (404) and (2111) respectively. The presence of dominant TiO<sub>2</sub> (112) in figure (4-11) for cpTi alloy, Suggests the formation of a thick oxide film on sample the oxide layer for cpTi alloy represent in TiO<sub>2</sub> as a result from coated with TiO<sub>2</sub> layer, heat treatment from annealing and exposer the sample for heat of plasma inside the sputtering system for long time all these lead to grow the fibrous strings TiO<sub>2</sub> towards up. The concentration of HA as single and triple layer was calculated corresponding to other material in thin film at time work (10 hours) using theoretical model TOBAS – XRD program as the following table.1, Concentration of apatite on cpTi alloy for single and Triple layer thin film.

**Table.3.** Concentration of Apatite in thin film

Alloys	Concentration of Apatite in thin film	
	Single layer	Triple layer
cpTi	81.29%	11.55%

The RF sputtering depositing particle with nano size as shown in table.4 the particle size calculated using Scherer equation in X-ray diffraction results

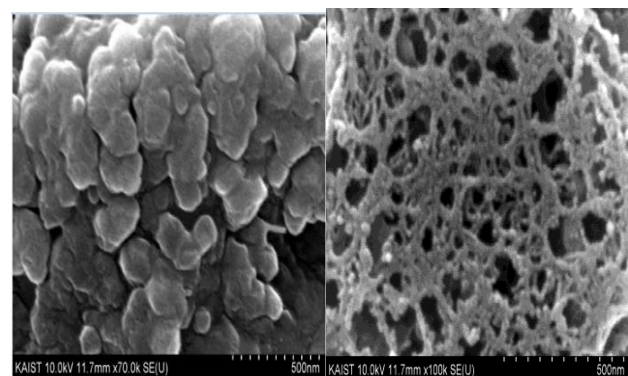
**Table 4.** The particle size HAp thin film coated using RF sputtering technique.

Sample thickness	Titanium cpTi alloy coated with HAp	crystal size (nm)
Single layer	HAp	22.0
Three layer	TiO <sub>2</sub> + Al <sub>2</sub> O <sub>3</sub> +HAp	26.6

The annealing temperature of the composite coating should be controlled to be not high due to the thermal decomposition of HAp phase. A crack-free and adhesive HAp/(TiO<sub>2</sub>+Al<sub>2</sub>O<sub>3</sub>) composite coating was then successfully fabricated using the RF deposition and reaction bonding process. The reaction bonding process promotes the coating's was improves the substrate's oxidation resistance during the heat treatment. In comparison with the single HAp coating, the triple layer HAp composite coating exhibits much higher bonding strength.

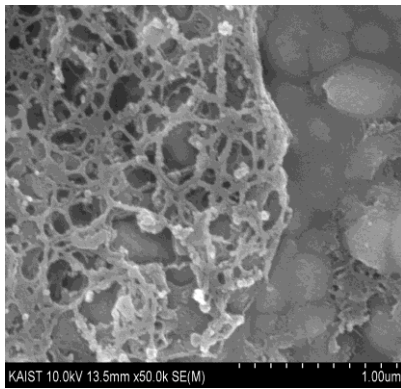
**B. SEM Scanning Electron Microscope & EDS Energy Dispersive X-ray Spectrometer.**

The surface morphology of single and triple HAp coating fabricated under the same conditions is shown in figure (2) and figure (3) as comparison. From figure(3-a and b), no pores were observed from the surface of the composite coating; while for the single HAp coating shown in figure(2), numerous pores were found because of the firing shrinkage during annealing or coated due to different in thermal expansion between Ti substrate and HAp. Figure (3) shows that the composite coating was well sintered. It is obvious that particles in the composite coating bond with each other and grain size grows; however, for the single Hap coating shown in figure(2), most particles appear to remain stand-alone, bonding among the particles is not as full as in the composite coating and there is nearly no growth of grain size. It can be excluded that the sintering property is greatly improved by the addition of TiO<sub>2</sub> and Al<sub>2</sub>O<sub>3</sub> to form coating. The irregular shape of grains in the composite coating implies the presence of liquid phase during annealing process which is known to be beneficial in the mass transport and bonding among grains. The volume expansion associated with the oxidation reaction of Ti→TiO<sub>2</sub> and intimate bonding between mixing three layers partially compensates for the sintering shrinkage and prevents the formation of cracks.

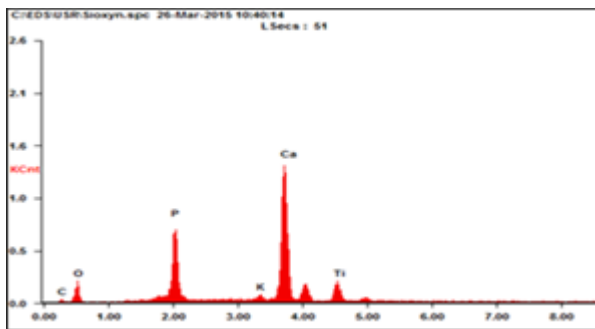


(a)

(b)



(c)



(d)

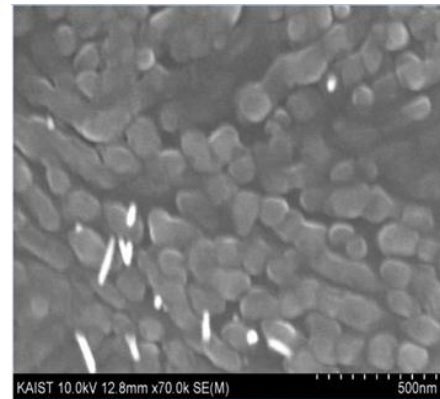
**Figure 2.** HAp single layer coated surface cpTi alloy (a, b and c) Top-view SEM image, (d) EDS

**Table.5.** EDS for cpTi coated with single layer HA high thickness.

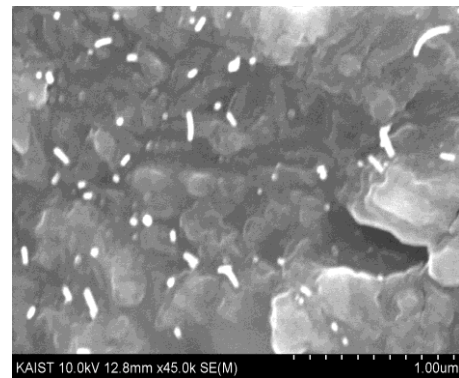
No. of experiment		1	2	3	4
Time of Work (hours)		2	4	7	10
Ti	Wt%	69.24	47.18	13.02	10.17
	At%	48.99	48.99	7.68	5.77
Al	Wt%	1.89	1.26	--	--
	At%	2.36	1.45	---	---
O	Wt%	18.24	21.29	26.22	24.47
	At%	38.55	42.55	46.31	41.65
Ca	Wt%	5.53	18.67	40.38	43.98
	At%	4.67	14.62	28.47	29.55
P	Wt%	1.57	6.97	14.82	15.84
	At%	1.72	6.93	13.52	13.78

From EDS figure (2-d) and table (5), the concentration of Ca, P increasing with increasing time of work this mean increasing in thickness of thin film. From figure (2-a,b and c), and figure (3-a and b) present the HA top view functional film are mostly spherical shape more uniform, were built by RF sputtering approximately the same and uniform distribution, the entire substrate surface covered by deposition when the thickness of thin film increasing the particle continues grow and agglomerates. From table 2 the RF sputtering depositing particle with nano size, small surface area and high force this lead to agglomerates for many particles and this agreement with results of XRD. The HA have phase

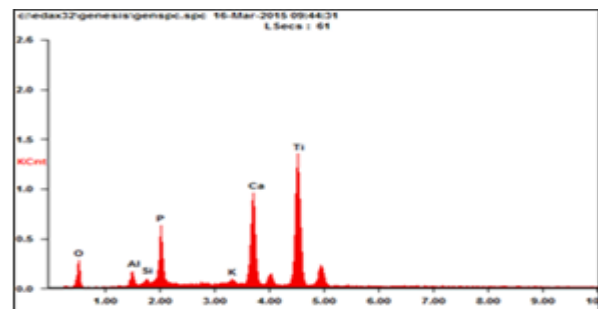
(hcp) and cpTi alloy containing single  $\alpha$  phase (hcp) so larger agglomerates can be seen into the deposition process on cpTi. [18]. From figure (3) there is a grow the fibrous strings  $TiO_2$  towards up and this agreement with results of XRD.



(a)



(b)



(c)

**Figure 3** ( $TiO_2-Al_2O_3-HA$ ) layers coated surface cpTi alloy (a and b) Top-view SEM image, (c)EDS.

**Table.6.** EDS for cpTi coated with triple layer HA.

No. of experiment		1	2	3
Time of Work (hours)		2	4	7
Ti	Wt%	74.4	46.65	43.37
	At%	55.0	29.6	27.22
Al	Wt%	1.38	7.28	2.49
	At%	1.82	3.67	2.77
O	Wt%	15.84	23.4	23.4
	At%	35.06	44.44	44.44

Ca	Wt%	5.49	16.48	12.49
	At%	4.85	19.61	14.71
P	Wt%	2.87	7.28	3.26
	At%	3.28	8.24	8.0

From EDS table (6), the concentration of Ca, P increasing with increasing time of work this mean increasing in thickness of thin film ,but the concentration of Ca, P lower than in single layer. By using alpha optical microscopy to measure the thickness thin film with time deposition time of work 10 hours , $TiO_2 + Al_2O_3 + HA = 1.37 \mu m$ , for single layer  $HA = 598nm$  .From fig 3(a and b) one can see intimate bonding between the HA layer and the  $Al_2O_3$  [15], low porosity no cracks or delamination phenomena were observed at the interface. The HA deposition as third layer have narrow size distribution with uniform grain size corresponding to the crystallinity improvement, no pours this mean that the  $Al_2O_3$  and HA work to cover the pours. The low concentration in HA from results of EDS table 6 and TOBAS table 3 because intercept and new bound between third layer HA and second layer  $Al_2O_3$ . The chemical compositions of the composite coating were determined through EDS element analysis. Relating spectrum is shown in figure (3-c) a concentration weight Ca, P increasing with time of working sputtering. The results show that elements Al, Ca, P and O are all present in the composite coating, which confirms that of HA and Al under the present condition is feasible.

### C. X-ray Photoelectron Spectrometer XPS

The behaviour XPS high spectrum for triple layer HA coated as shown in figure 4,

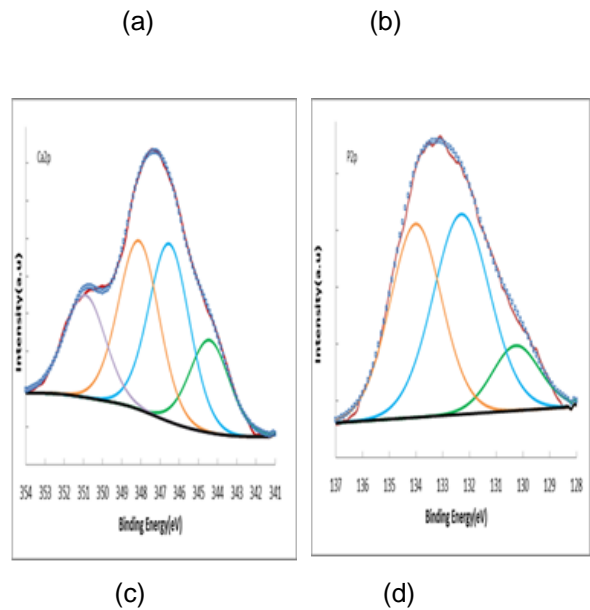
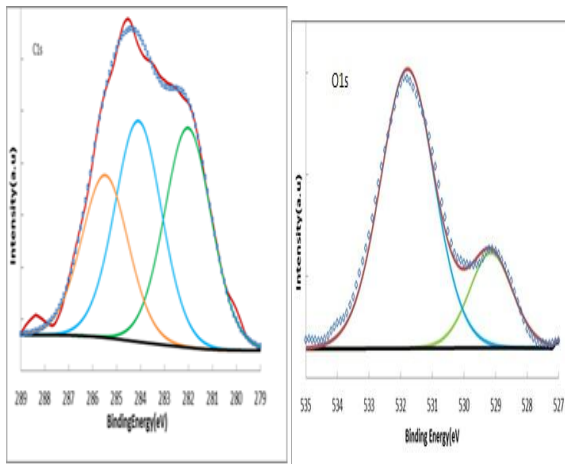


**Figure 4.** XPS spectra high resolution of the first-layer coating HA C1s spectra for triple layer HAp:(a) C1s , (b) O1s , (c) Ca 2p and (d) P 2p

From fig. 4 (a), it is seen that the deconvolution of C1s spectrum for triple layer HAp consists of three sub peaks: the first peaks at 284.43 due to external adventitious carbon, the second peaks 285.20 is assigned to  $C_{10}H_8$  .the third peak for a single layer at 282.22 eV is attributed to  $(C_6H_5)_2PCH_2P$   $(C_6H_5)_2$  .All the findings were found to be in good agreement with the NIST XPS database and refs. [19] [20]. Fig. 4 (b) The deconvolution of the O 1s spectrum for triple layer HAp contains two oxygen species: first two components at 529.14 eV, 531.78eV are attributed to same phase CaO phase respectively in accordance with the NIST XPS database and literature [3] [21]. The Ca2p in fig.4(c) has four sub peaks 346.52, 348.10, 350.90 are assigned to CaP the 344.42 eV correspond to chemical space Ca 2p<sub>1/2</sub> and can be attributed to chemical phosphate material CPM [19] [20] and Table7 show the XPS spectrum analysis high resolution of HA for triple layer.

Table7 show the XPS spectrum analysis high resolution of HA for triple layer.

Samples	Line	Bonding states	Binding Energy(eV)	FWHM(eV)	Percentages of component (%)
cpTi+HAp(S.L)	C1s	(C6H5)2PCH2P(C6H5)2	282.22	2.32	36.49
		C	284.43	1.500	45.95
		C10H8	285.20	1.149	19.41
	O1s	CaO	529.14	1.60	21.46
		CaO	531.78	2.00	78.54
	Ca 2p	Ca	344.42	2.44	16.81
		CaP	346.52	2.50	33.06
		CaP	348.10	2.48	31.13
	P 2p	CaP	350.90	2.50	18.99
		(C6H5)2PCH2P(C6H5)2	130.99	1.04	8.90
P		132.84	2.36	38.06	
		CaHPO4	133.85	2.36	53.04

Consider in the NIST XPS database. The P 2p

main peak are divided into three sub peaks, at BE values of 130.99eV is assigned to (C6H5)2PCH2P(C6H5)2 corresponding to NIST XPS database and 132.84 is identified to be P, the last sub peaks at binding energies 133.85 are attributed to CaHPO, all these peaks are attributed the pyrophosphate groups [3].

#### D- Corrosion

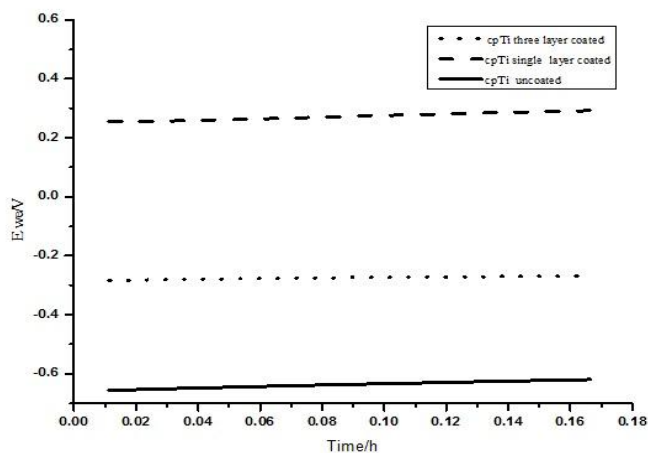
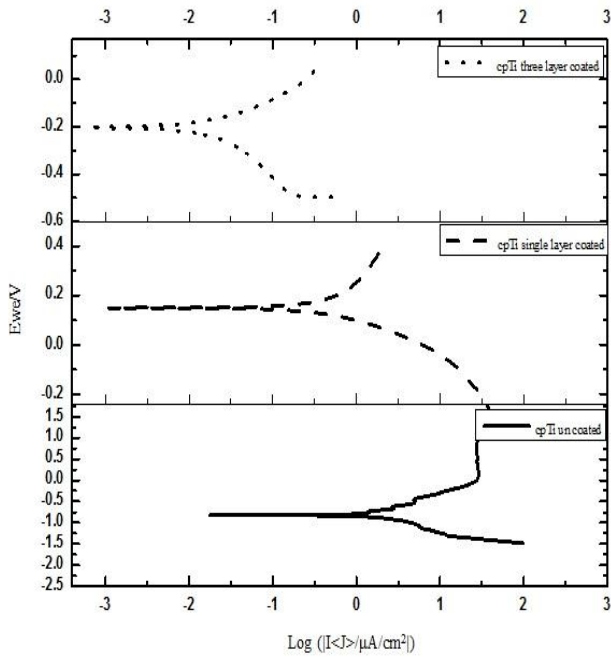


Figure 5. The steady-state OCP for cpTi alloy uncoated and coated as hree layer





**Figure.6.** The steady-state OSV for cpTi alloy uncoated and coated as single and three layer

**Table 8.** cpTi alloy uncoated and coated as single and three layer

Samples	$I_{corr}$ ( $\mu A/cm^2$ )	$E_{corr}$ (mV)	Corrosion ratio (mmpy)
cpTi uncoated	0.792	-650.351	$5.639 \times 10^{-3}$
cpTi single layer coated	0.065	210.365	$0.565 \times 10^{-3}$
cpTi three layer coated	0.009	-224.807	$78.33 \times 10^{-6}$

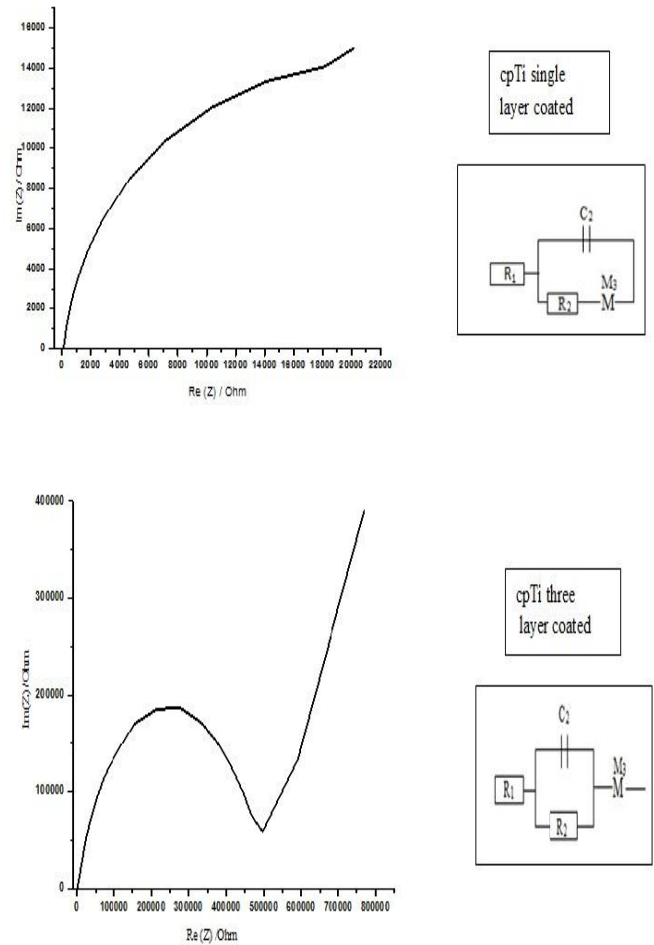


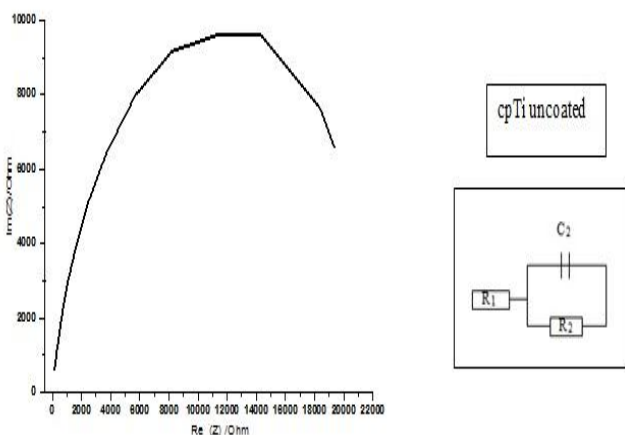
**Figure.7** The Nyquist impedance- EIS for cpTi alloy uncoated and coated as single and three layers

**Table 9.** The value of elements of equivalent circuits

The passive behaviour of cpTi uncoated and coated in SBF solution has been determined by a number of

Samples	$R_1$ ( $\Omega$ )	$R_2$ ( $\Omega$ )	C (F)	M ( $\Omega$ )
cpTi uncoated	60.57	23125	$12.33 \times 10^{-9}$	-----
cpTi single layer coated	80.68	30716	$45.88 \times 10^{-6}$	9492
cpTi three layer coated	1070	508276	$1.246 \times 10^{-6}$	514392

workers. This technique was used for evaluating corrosion parameters for different specimens with different surface coated as shown in table 8 and 9. Fig.5 show the techniques (OCP for cpTi alloy coated and uncoated, in general all sample are found quasi-steady state value ( $E_{we}$ ). The potential of coated samples drifts in the noble direction especially for





single later more than for three layers coated within 15 min. The potential positive shift of potential indicates the passivation layer increasing by coated but un depend on thickness because the thickness for three layer more than single layer .

From fig .6 the OSV for cpTi alloy uncoated and coated alloy. There are approximately agreement between the values of potential corrosion  $E_{corr}$  in table 8 from fig 5 and fig. 6 the OCV behaviour. From table 8, the value of  $I_{corr}$  for cpTi alloy coated as single layer  $0.065(\mu A/cm^2)$  is less than the value of cpTi alloy uncoated  $0.792(\mu A/cm^2)$  and more less than for three layer coated  $0.009(\mu A/cm^2)$  that is mean improvement in passivation layer after coated lead to reduce the value of  $I_{corr}$ . Also we can see that from Corrosion ratio (mmpy) in table 8, the Corrosion ratio (mmpy) of (cpTi coated single layer/ cpTi un coated)= 10 tims and for (cpTi coated three layer / cpTi un coated)=71 tims .

Fig .7 the (EIS). An equivalent electronic circuit model for the electrochemical system was suggested and the impedance data were obtained by fitting the experimental data to an appropriate proposed circuit model open circuit stability of the passive film in SBF solutions. Equivalent circuit (Randle's circuit) depicting the corrosion model. Which compromises the

Polarization resistance ( $R_2$ ) in parallel with the capacitance of coated layer ( $C_2$ ), in series with the resistance of solution ( $R_1$ ), was used for the EIS model.  $R_1$  is the uncompensated resistance of the electrolyte between the working and the reference electrode;  $R_2$  is the polarization resistance or the charge transfer resistance at the working electrode/electrolyte interface, related to the rate of corrosion reactions at the passive domain;  $C_2$  is the specific double-layer capacitance at the working electrode/electrolyte interface. From fig. 7 this form of equivalent circuit means there are porosities for cpTi uncoated and coated ,the natural oxide layer for cpTi uncoated have porosity , after coated with single layer HAp there are internal impedance add to equivalent circuite represent in M. The porosities continue present but with little effect , from Nyquist impedance curve EIS it cover more space compared with uncoated .For three layer cp Ti coated , Nyquist impedance curve EIS it cover more space area and appear new outer impedance in equivalent represent in M which connected in series with circuit of  $C_2$  and  $R_2$ . Outer resistance belong to three layers with value greater than the value of M in single layer. The surface modified by RF sputtering technique improvement the resistance corrosion of surface and for three layers better than from single layer.

#### IV. CONCLUSIONS

Hydroxyapatite sputtering has been achieved successfully to form single HA and triple HAp/ $Al_2O_3/TiO_2$  layers coating on cpTi alloy. By applying good working condition, the thickness of thin film increasing with increasing the time deposition without cracks. The RF sputtering process reduces

the particles from micro size to nano scale which is similar to the hydroxyapatite in human body. The three layer coating is better than single layers because different atoms create new bonds which play important falters to reduce the porosity , crack formation and improve cross ion resistance and finally give the surface high active biocompatibility.

#### REFERENCE

- [1] E. Fuchs, K. Mandel, S. Bouazza, a Rosin, and E. Weiss, "Surface Modification of Porous Titanium Composites Obtained by Different Processing Methods," vol. 4, pp. 1–7, 2009.
- [2] H. W. Kim, Y. H. Koh, L. H. Li, S. Lee, and H. E. Kim, "Hydroxyapatite coating on titanium substrate with titania buffer layer processed by sol-gel method," *Biomaterials*, vol. 25, no. 13, pp. 2533–2538, 2004.
- [3] V. Khalili, "Titanium Oxide ( $TiO_2$ ) Coatings on NiTi Shape Memory Substrate Using Electrophoretic Deposition Process," *Int. J. Eng.*, vol. 26, no. 7 (A), pp. 707–712, 2013.
- [4] S. Yamaguchi, T. Yabutsuka, M. Hibino, and T. Yao, "Development of novel bioactive composites by electrophoretic deposition," *Mater. Sci. Eng. C*, vol. 29, no. 5, pp. 1584–1588, 2009.
- [5] I. Zhitomirsky and L. Gal-Or, "Electrophoretic deposition of hydroxyapatite," *J. Mater. Sci. Mater. Med.*, vol. 8, no. 4, pp. 213–219, 1997.
- [6] L. Pawlowski, "Thick Laser Coatings: A Review," *J. Therm. Spray Technol.*, vol. 8, no. 2, pp. 279–295, 1999.
- [7] X. Zhao, X. Liu, C. Ding, and P. K. Chu, "In vitro bioactivity of plasma-sprayed  $TiO_2$  coating after sodium hydroxide treatment," *Surf. Coatings Technol.*, vol. 200, no. 18–19, pp. 5487–5492, 2006.
- [8] Y. L. Wenjie ZHANG, "Propertioesof  $TiO_2$  thin films prepeard bymagntron sputtering," *J. Biomed. Mater. Res. Part B Appl. Biomater.*, no. 78B, pp. 146–152, 2006.
- [9] K. Okimura, "Low temperature growth of rutile  $TiO_2$  films in modified rf magnetron sputtering," *Surf. Coatings Technol.*, vol. 135, no. 2–3, pp. 286–290, 2001.
- [10] J. G. C. Wolke, J. P. C. M. Van Der Waerden, K. De Groot, and J. a. Jansen, "Stability of radiofrequency magnetron sputtered calcium phosphate coatings under cyclically loaded conditions," *Biomaterials*, vol. 18, no. 6, pp. 483–488, 1997.
- [11] Y. L. and F. Wenjie ZHANG, "properties of  $TiO_2$  thin films prepared by magntron sputtering," *Mater. Sci. Technol*, vol. 18, 2002.

- [12] J. Long, L. Sim, S. Xu, and K. Ostrikov, "Reactive plasma-aided RF sputtering deposition of hydroxyapatite bio-implant coatings," *Chem. Vap. Depos.*, vol. 13, no. 6–7, pp. 299–306, 2007.
- [13] S. Xu, J. Long, L. Sim, C. H. Diong, and K. Ostrikov, "RF plasma sputtering deposition of hydroxyapatite bioceramics: Synthesis, performance, and biocompatibility," *Plasma Process. Polym.*, vol. 2, no. 5, pp. 373–390, 2005.
- [14] D. Shi, Ed., *Introduction to Biomaterials*. Singapore: World Scientific, 2006.
- [15] Z.-C. Wang, "Fabrication and characterization of HAp /Al<sub>2</sub>O<sub>3</sub> composite coating on titanium substrate," *J. Biomed. Sci. Eng.*, vol. 01, no. 03, pp. 190–194, 2008.
- [16] L. Mohan, D. Durgalakshmi, M. Geetha "Electrophoretic deposition of nanocomposite (HAp + TiO<sub>2</sub>) on titanium alloy for biomedical applications" *Ceramics International* 38 (2012) 3435–3443
- [17] S.J.Ding, "Properties and immersion behaviour of magnetron –sputtered multi-layered hydroxyapatite/titanium composite coatings" *Biomaterials*, vol.24,no.23,pp.4233-4238,2003.
- [18] W. So54 G fdboyejo ,Mechanical Properties of Engineered Materials.New York:Marcel Dekker AG,2003.
- [19] R.J.Chung ,M.F.Hsieh,R.N.Panda,and T.S.Chin,"Hydroxyapatite layers deposited from aqueous solutions on hydrophilic silicon substrate," *Surf. Coatings Technol.*, vol. 165 ,nono.2,pp.194-200,2003.
- [20] H. Shin, J. Jung, S. Kim, and W. Lee, "XPS Analysis on Chemical Properties of Calcium Phosphate Thin Films and Osteoblastic HOS Cell Responses," 2006.
- [21] C. C. Chusuei, D. W. Goodman, M. J. Van Stipdonk, D. R. Justes, and E. a Schweikert, "Calcium Phosphate Phase Identification Using XPS and Time-of-Flight Cluster SIMS.," *Anal. Chem.*, vol. 71, no. 1, pp. 149–153, 1999.